

# A Steklov-Poincaré Approach to Solve the Inverse Problem in Electrocardiography

Nejib Zemzemi

INRIA Bordeaux Sud-Ouest, France

## Abstract

*In the cardiac electrophysiology imaging community the most widely used approach to solve the inverse problem is the least square formulation with different Thikhonov regularizations. Clinicians are not yet fully satisfied by the technology that solves the inverse problem. Reformulating the inverse problem could bring new techniques to solve it. In this paper we use the Steklov-Poincaré formulation of the Cauchy problem in order to solve the inverse problem in electrocardiography imaging. We present in this work the technique and an algorithm of gradient descent. We also show numerical results based on simulated synthetic data.*

## 1. Introduction

The inverse problem in cardiac electrophysiology also known as electrocardiography imaging (ECGI) is a procedure that allows reconstructing the potential on the outer surface of the heart (epicardium) from potential measurements on the surface of the torso. This non-invasive technology and other similar techniques like the electroencephalography imaging are highly demanded by medical industries and clinicians. ECGI allows a better spacial targeting of cardiac arrhythmias and thus it helps to make more accurate clinical interventions. However, the non-invasive reconstruction of the epicardial potential is not straitforward. The difficulty in the reconstruction of electrical potential on the heart surface comes from the ill posedness of the mathematical problem behind the reconstruction. Different works treated this problem [1–3] based on boundary element method for the discretization and Thikhonov regularization techniques to ensure the well posedness of the mathematical problem. None of the methods in the literature have been shown to work perfectly. In this paper we propose an other approach of treating the inverse problem in electrocardiography based on the Steklov-Poincaré formulation of the Cauchy problem [4]. In order to test this approach we first simulate the forward problem based on the state of the art bidomain model. This

allow as to generate electrical potentials in the heart and in the torso. We then extract ECG data from the torso surface and use it as input for the inverse problem. The solution of the inverse problem is then compared the synthetical electrical potential on the heart surface.

## 2. Methods

In this section we present the mathematical formulations and numerical methods that are used in this paper to simulate the forward and to solve inverse problem. In paragraph 2.1, we present the mathematical models and methods used in order to simulate the electrical potential in the heart and the torso. In paragraph 2.2, we present the mathematical formulation and the algorithm used to solve the inverse problem.

### 2.1. Forward problem

The bidomain equations were used to simulate the electrical activity of the heart and extracellular potentials in the whole body (see *e.g.* [5–7]). These equations in the heart domain  $\Omega_H$  are given by:

$$\begin{cases} A_m(C_m \dot{V}_m + I_{ion}(V_m, \mathbf{w})) - \operatorname{div}(\boldsymbol{\sigma}_i \nabla V_m) \\ \quad \quad \quad = \operatorname{div}(\boldsymbol{\sigma}_i \nabla u_e) + I_{stim}, & \text{in } \Omega_H, \\ -\operatorname{div}((\boldsymbol{\sigma}_i + \boldsymbol{\sigma}_e) \nabla u_e) = \operatorname{div}(\boldsymbol{\sigma}_i \nabla V_m), & \text{in } \Omega_H, \\ \dot{\mathbf{w}} + \mathbf{g}(V_m, \mathbf{w}) = 0, & \text{in } \Omega_H, \\ \boldsymbol{\sigma}_i \nabla V_m \cdot \mathbf{n} = -\boldsymbol{\sigma}_i \nabla u_e \cdot \mathbf{n}, & \text{on } \Sigma. \end{cases} \quad (1)$$

The state variables  $V_m$  and  $u_e$  stand for the transmembrane and the extra-cellular potentials. Constants  $A_m$  and  $C_m$  represent the rate of membrane surface per unit of volume and the membrane capacitance, respectively.  $I_{stim}$  and  $I_{ion}$  are the stimulation and the transmembrane ionic currents. The heart-torso interface is denoted by  $\Sigma$ . The intra- and extracellular (anisotropic) conductivity tensors,  $\boldsymbol{\sigma}_i$  and  $\boldsymbol{\sigma}_e$ , are given by  $\boldsymbol{\sigma}_{i,e} = \sigma_{i,e}^t \mathbf{I} + (\sigma_{i,e}^l - \sigma_{i,e}^t) \mathbf{a} \otimes \mathbf{a}$ , where  $\mathbf{a}$  is a unit vector parallel to the local fibre direction and  $\sigma_{i,e}^l$  and  $\sigma_{i,e}^t$  are, respectively, the longitudinal and transverse conductivities of the intra- and extra-cellular media. The field

of variables  $w$  is a vector containing different chemical concentrations and various gate variables. Its time derivative is given by the vector of functions  $g$ .

The precise definition of  $g$  and  $I_{\text{ion}}$  depend on the electrophysiological transmembrane ionic model. In the present work we make use of one of the biophysically detailed human ventricular myocyte model [8].

Figure 1 provides a geometrical representation of the domains considered to compute extracellular potentials in the human body. In the torso domain  $\Omega_T$ , the electrical potential  $u_T$  is described by the Laplace equation.

$$\begin{cases} \operatorname{div}(\sigma_T \nabla u_T) = 0, & \text{in } \Omega_T, \\ \sigma_T \nabla u_T \cdot \mathbf{n}_T = 0, & \text{on } \Gamma_{\text{ext}}. \end{cases} \quad (2)$$

where  $\sigma_T$  stands for the torso conductivity tensor and  $\mathbf{n}_T$  is the outward unit normal to the torso external boundary  $\Gamma_{\text{ext}}$ .

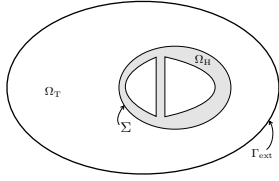


Figure 1. Two-dimensional geometrical description: heart domain  $\Omega_H$ , torso domain  $\Omega_T$  (extramyocardial regions), heart-torso interface  $\Sigma$  and torso external boundary  $\Gamma_{\text{ext}}$ .

The heart-torso interface  $\Sigma$  is supposed to be a perfect conductor. Then we have a continuity of current and potential between the extra-cellular myocardial region and the torso region.

$$\begin{cases} u_e = u_T, & \text{on } \Sigma, \\ (\sigma_e + \sigma_i) \nabla u_e \cdot \mathbf{n}_T = \sigma_T \nabla u_T \cdot \mathbf{n}_T, & \text{on } \Sigma. \end{cases} \quad (3)$$

Other works [9–11] consider that the electrical current does not flow from the heart to the torso by assuming that the heart is isolated from torso. This approximation is appealing in terms of computational cost because it uncouples the Laplace equation (2) in the torso from the bidomain equations in the heart (1), which allows to reduce the size of the linear system to solve. It is even more appealing when the interest is only on the ECG computation, in that case the ECG solution could be an "off line" matrix vector multiplication after solving the bidomain equation, details about computing the transfer matrix could be found in [12]. Although this approach is very appealing in terms of computational cost, numerical evidence has shown that it can compromise the accuracy of the ECG signals (see e.g. [5, 11, 13]). Thus, in order to accurately compute ECGs we consider the the state-of-the-art heart-torso full coupled electrophysiological problem (1)-(3) representing

the cardiac electrical activity from the cell to the human body surface.

## 2.2. Inverse problem

The inverse problem in electrocardiography imaging (ECGI) is a technique that allows to construct the electrical potential on the heart surface  $\Sigma$  from data measured on the body surface  $\Gamma_{\text{ext}}$ . We assume that the electrical potential is governed by the diffusion equation in the torso as shown in the previous paragraph. For a given potential data  $T$  measured on the body surface  $\Gamma_{\text{ext}}$ , the goal is to find  $u_e$  on  $\Sigma$  such that the potential data in the torso domain satisfies

$$\begin{cases} \operatorname{div}(\sigma_T \nabla u_T) = 0, & \text{in } \Omega_T, \\ \sigma_T \nabla u_T \cdot \mathbf{n} = 0, \text{ and } u_T = T, & \text{on } \Gamma_{\text{ext}}, \\ u_T = ?, & \text{on } \Sigma. \end{cases} \quad (4)$$

In order to find  $u_e$ , for a given boundary value distribution  $\lambda$  on  $\Sigma$ , we propose to define  $u_D(\lambda)$  and  $u_N(\lambda)$  as follows,

$$\begin{cases} \operatorname{div}(\sigma_T \nabla u_D(\lambda)) = 0, & \text{in } \Omega_T, \\ u_D(\lambda) = T, & \text{on } \Gamma_{\text{ext}}, \\ u_D(\lambda) = \lambda, & \text{on } \Sigma. \end{cases} \quad (5)$$

$$\begin{cases} \operatorname{div}(\sigma_T \nabla u_N(\lambda)) = 0, & \text{in } \Omega_T, \\ \sigma_T \nabla u_N(\lambda) \cdot \mathbf{n} = 0, & \text{on } \Gamma_{\text{ext}}, \\ u_N(\lambda) = \lambda, & \text{on } \Sigma. \end{cases} \quad (6)$$

Let's define the cost function as follows

$$J(\lambda) = \frac{1}{2} \int_{\Omega_T} (\nabla u_D(\lambda) - \nabla u_N(\lambda))^2. \quad (7)$$

This means that if  $J(\lambda) = 0$ , we have  $\nabla u_D(\lambda) = \nabla u_N(\lambda)$  in the whole domain  $\Omega_T$  and then  $\nabla u_D(\lambda) \cdot \mathbf{n} = \nabla u_N(\lambda) \cdot \mathbf{n}$  on the boundary and in particular on  $\Gamma_{\text{ext}}$ . Therefore, since  $u_D = u_N = \lambda$  on  $\Sigma$  and by uniqueness of the Laplace solution, we obtain that  $u_D(\lambda) = u_N(\lambda)$  in all the domain  $\Omega_T$ . Which means that both of solutions  $u_D(\lambda)$  and  $u_N(\lambda)$ , satisfy both Neumann and Dirichlet boundary conditions on  $\Gamma_{\text{ext}}$  at the same time. This means that  $\lambda$  is the solution of the inverse problem.

Our goal is to minimize the cost function  $J$ . Since we are able to calculate the gradient of the cost function, we can use a gradient descent method. For any test function  $\phi$ , the gradient of  $J$  reads:

$$\begin{aligned} \langle \nabla_\lambda J(\lambda), \phi \rangle &= \left\langle \int_{\Omega_T} (\nabla u_D - \nabla u_N) \nabla_\lambda (\nabla u_D - \nabla u_N), \phi \right\rangle \\ &= \left\langle \int_{\Omega_T} (\nabla u_D - \nabla u_N) \nabla_\lambda (\nabla u_D), \phi \right\rangle \\ &\quad - \left\langle \int_{\Sigma} (\nabla u_D - \nabla u_N) \nabla_\lambda (\nabla u_N), \phi \right\rangle \end{aligned} \quad (8)$$

Applying the Green formula on both terms we find

$$\nabla_{\lambda} J(\lambda) = (\nabla u_D - \nabla u_N) \cdot \mathbf{n} \quad (9)$$

For a given initial guess  $\lambda$ , we compute the incomplete boundary condition following the algorithm 1.

---

**Algorithm 1** Algorithm

---

```

 $\lambda = 0$ 
for  $i = \text{first time step to last time step}$  do
  load the known boundary data  $u_T(t_i)_{/\Gamma_{\text{ext}}}$ 
  compute  $u_D(\lambda)$ 
  compute  $u_N(\lambda)$ 
  compute  $\nabla_{\lambda} J(\lambda) = (\nabla u_D - \nabla u_N) \cdot \mathbf{n}$ 
  while ( $\|\nabla_{\lambda} J(\lambda)\| > \text{tolerance}$ ) do
     $\lambda \leftarrow \lambda - \delta * \nabla_{\lambda} J(\lambda)$ 
    compute  $u_D(\lambda)$ 
    compute  $u_N(\lambda)$ 
    compute  $\nabla_{\lambda} J(\lambda) = (\nabla u_D - \nabla u_N) \cdot \mathbf{n}$ 
  end while
  save  $u_T(t_i)_{/\Sigma} = \lambda$ 
end for

```

---

In practice, putting  $\lambda = 0$  out of the time loop reduces the number of iterations in the while loop. This could be explained by the fact that the solution at time  $t + \delta_t$  is closer to the solution at time  $t$  then it is to zero.

### 3. Numerical results

In this paragraph we show numerical results for direct and inverse problem obtained using the numerical methods presented above. For the sake of conciseness we perform simulations on the volumes between three concentric spheres. The volume between the small and the medium sphere represents the heart domain and the volume between the medium and the large spheres represents the torso. The epicardium is given by the medium sphere while the body surface is given by the largest sphere. In Figure2, we plot simulations of the forward problem where we stimulate the heart in tow opposite locations. The figure represents snapshots of the electric potential in the depolarization phase (four first images) and depolarization phase in the four last images. In order to test the inverse problem resolution approach given by algorithm 1, we extract from the direct solution the values of the electrical potential on the torso (on the external sphere) and we try to recover the value of the electrical potential on the epicardial surface. In Figures 3, we show comparison between the exact potential (left column) in the torso and the inverse solution (right column) using algorithm 1. The first tow rows contain the comparison at depolarization phase (times 10 and 25 ms), we can see that the wave front is captured and both of stimuli positions are clearly identified from the inverse

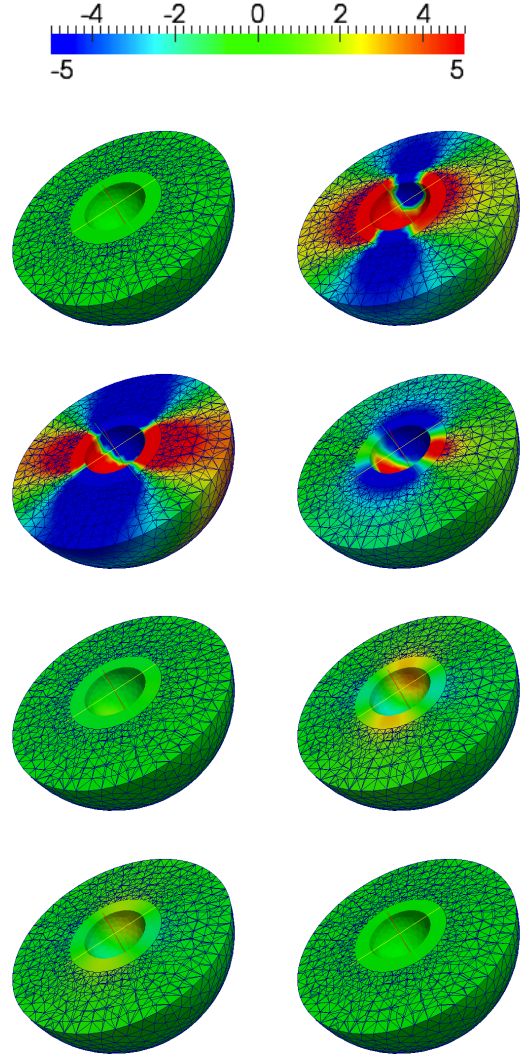


Figure 2. Snapshots of the extracellular potential (small sphere) and BSP (large sphere) at times 0, 4, 20, 35, 40, 220, 300, 400 ms (from left to right and from top to bottom). The color bar scale is in mV.

solution. The two last rows in figure 3, represent the forward (left) and the inverse (right) solutions at the repolarization phase. The repolarization wave front is clearly and the spatial distribution of the electrical potential seems to be accurate.

### 4. Discussion

In the present work we showed an alternative to the least square approach which has been intensively used in the electrocardiography imaging community, this approach does not need the computation of a transfer matrix. It uses a gradient descent method to recover the electrical potential at the external heart boundary. The weakness of gradi-

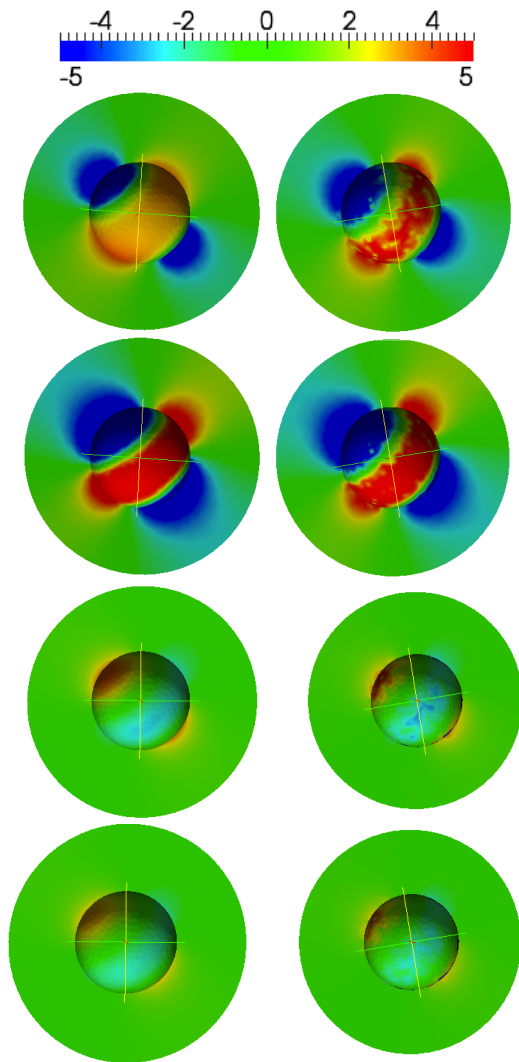


Figure 3. Comparison between exact solution (left column) and inverse solution (right column). Snapshots of torso potential at times 10, 25, 300 and 310 ms (from top to bottom). The color bar scale is in mV.

ent descent methods in general is that algorithm could fall in a local minimum rather than the global optimum. This problem could be tackled by combining the gradient descent method with global optimum algorithm like genetic algorithms and evolution strategy algorithms.

## 5. Conclusion

In this paper we presented a new approach to tackle the inverse problem in cardiac electrophysiology. We used an ECG simulator to construct a synthetic data of body surface potential. This synthetic data is obtained from numerical simulations, based on a 3D mathematical model of the ECG involving a mathematical description of the electrical activity of the heart and the torso. We then used

the Steklov-Poincaré formulation of the Cauchy problem, and used a gradient descent method to solve the inverse problem. Numerical simulations show that this method is able to localize the wave front generated by two stimuli in the heart both in the depolarization and in the repolarization phases. In future works this method would be tested on clinical data of electrical potential, with anatomically accurate heart and torso geometries.

## References

- [1] Zakharov E, Kalinin A. Algorithms and numerical analysis of dc fields in a piecewise-homogeneous medium by the boundary integral equation method. *Computational Mathematics and Modeling* 2009;20(3):247–257.
- [2] Ghosh S, Rudy Y. Application of  $l_1$ -norm regularization to epicardial potential solution of the inverse electrocardiography problem. *Annals of Biomedical Engineering* 2009; 37(5):902912.
- [3] Denisov A, Zakharov E, Kalinin A, Kalinin V. Numerical methods for some inverse problems of heart electrophysiology. *Differential Equations* 2009;45(7):1034–1043.
- [4] Belgacem FB, El Fekih H. On Cauchy's problem: I. a variational Steklov-Poincaré theory. *Inverse Problems* 2005; 21(6):1915.
- [5] Pullan A, Buist M, Cheng L. Mathematically modelling the electrical activity of the heart. From cell to body surface and back again. World Scientific, 2005.
- [6] Sundnes J, Lines G, Cai X, Nielsen B, Mardal KA, Tveito A. Computing the electrical activity in the heart. Springer-Verlag, 2006.
- [7] Tung L. A bi-domain model for describing ischemic myocardial D-C potentials. Ph.D. thesis, MIT, 1978.
- [8] Ten Tusscher K, Panfilov A. Cell model for efficient simulation of wave propagation in human ventricular tissue under normal and pathological conditions. *Physics in medicine and biology* 2006;51:6141.
- [9] Clements J, Nenonen J, Li P, Horacek B. Activation dynamics in anisotropic cardiac tissue via decoupling. *Annals of Biomedical Engineering* 2004;2(32):984–990.
- [10] Potse M, Dubé B, Gulrajani M. ECG simulations with realistic human membrane, heart, and torso models. In *Proceedings of the 25th Annual International Conference of the IEEE EMBS*. 2003; 70–73.
- [11] Lines GT, Buist ML, Grotttum P, Pullan AJ, Sundnes J, Tveito A. Mathematical models and numerical methods for the forward problem in cardiac electrophysiology. *Comput Visual Sci* 2003;5(4):215–239.
- [12] Zemzemi N. Étude théorique et numérique de l'activité électrique du cœur: Applications aux électrocardiogrammes. Ph.D. thesis, Université Paris XI, 2009. <http://tel.archives-ouvertes.fr/tel-00470375/en/>.
- [13] Boulakia M, Cazeau S, Fernández M, Gerbeau J, Zemzemi N. Mathematical modeling of electrocardiograms: a numerical study. *Annals of biomedical engineering* 2010; 38(3):1071–1097. ISSN 0090-6964.